



Contrasting the mechanical and metallurgical properties of laser welded and gas tungsten arc welded S500MC steel

Saleh Meiabadi¹ · Fardin Nematzadeh² · Kianoosh Kornokar² · Hossein Mostaan² · Mahmoud ShamsBorhan³ · Rasoul Khandan⁴ · Vincent Demers¹ · Jonathan Lawrence⁵ · Mahmoud Moradi⁶

Received: 29 March 2023 / Accepted: 20 June 2023
© The Author(s) 2023

Abstract

S500MC steel is a grade of high-strength low-alloy steel (HSLA) which is widely used in the automotive industry and for agricultural machinery and equipment. Considering properties of this alloy, selection of the welding process and parameters becomes essential to ensure that HSLA assemblies meet specific service requirements. In this work, mechanical and metallurgical properties of S500MC steel produced by autogenous laser beam welding (LBW) and automatic gas tungsten arc welding (GTAW) were compared. Tensile testing, metallography, hardness testing, and fractographic analysis were performed on the welded specimens, revealing that the heat input by these welding processes caused significant microstructural changes within the joints. In LBW samples, the heat input about 10 times lower than that in GTAW produced a finer microstructure, narrower fusion zone width, and smaller heat-affected zone. All fractures of the GTAW specimens occurred in the base metal, while all fractures of the LBW specimens occurred in the weld zone, both regardless of the heat input. GTAW joints exhibited higher mechanical properties (even higher than those obtained in the base metal) as compared to LBW joints.

Keywords High-strength low-alloy steel · Fiber laser welding · GTAW welding · Microstructure · Mechanical properties

1 Introduction

The application of advanced welding methods in the industry is increasing on a daily basis because of the reduced

processing time, energy, and running costs in the production process. Laser beam welding (LBW) and gas tungsten arc welding (GTAW) both using shielding protective gas can be good alternatives to provide quality welding in some projects of industrial applications compared to other more

Recommended for publication by Commission IV - Power Beam Processes.

- ✉ Saleh Meiabadi
mohammadsaleh.sheikhmohammadmeiabadi.1@ens.etsmtl.ca
- ✉ Fardin Nematzadeh
f-nematzadeh@araku.ac.ir
- ✉ Mahmoud Moradi
Mahmoud.Moradi@northampton.ac.uk
- Kianoosh Kornokar
kornokarkianosh@gmail.com
- Hossein Mostaan
h-mostaan@araku.ac.ir
- Mahmoud ShamsBorhan
m.shamsborhan@gmail.com
- Vincent Demers
vincent.demers@etsmtl.ca
- Jonathan Lawrence
jonathan.lawrence@uws.ac.uk

- ¹ Department of Mechanical Engineering, École de Technologie Supérieure, 1100 Notre-Dame West, Montreal, QC H3C 1K3, Canada
- ² Department of Materials and Metallurgical Engineering, Faculty of Engineering, Arak University, Arak 38156-88349, Iran
- ³ Department of Mechanical Engineering, University of Zakho, Zakho, Kurdistan Region, Iraq
- ⁴ College of Engineering and Physical Sciences, Aston University, Birmingham B4 7ET, UK
- ⁵ School of Computing, Engineering & Physical Sciences, University of the West of Scotland (UWS), Paisley Campus, Paisley PA1 2BE, UK
- ⁶ Faculty of Arts, Science and Technology, University of Northampton, Northampton NN1 5PH, UK

traditional processes bringing lower efficiencies, clamping requirements, and difficulties associated with robotization and automation. LBW is one of the most versatile and flexible liquid-state joining methods that can be used in the realization of the production process of industrial products. In this respect, welding using a laser heat source installed on a computer numerical control (CNC) system is known as an advanced process [1]. The most popular advantages of laser welding systems include accuracy, higher speed, low heat input, minimized residual stress, successful welding of heat-sensitive parts, high automation capability, less preparation steps, and high potential for welding dissimilar metals [2, 3]. In the GTAW process, the weld pool is obtained by an electric arc between a non-consumable tungsten electrode or its alloy and the workpiece. In these two processes, the molten metal area may be protected using shielding gas. Generally speaking, LBW produces narrower width of the heat-affected zone (HAZ) and significantly less distortion as compared to GTAW [4, 5].

HSLA steels are valued for ability to maintain good weldability and formability while still offering superior strength derived from controlled thermomechanical manufacturing process. Controlling the rolling process at certain temperatures ends up ultra-fine microstructure and improved mechanical properties [6]. In addition, vanadium and titanium elements form carbide and nitride particles in the alloy acting as grain growth barriers which prevent grain growth process during hot forming, ultimately resulting in both an increase in strength and toughness [7, 8]. The cold workability and bend formability in this steel have made it used in light weight structures and vehicles, including in the manufacture of chassis and panels of machines and other uses such as bridges and pressure tanks [9, 10]. A number of studies on the fusion welding of S500MC steel have been carried out, especially in the last 10 years, using different sources of heat. The effects of different gas metal arc welding (GMAW) conditions on the microstructure, hardness, and defects of such HSLA steel plate were investigated by Frih et al. [11]. Their microstructural analysis revealed very fine equiaxed grains at the weld zone, coarse grained in the HAZ near the weld boundary, partially refine grained zone on the middle of the HAZ, as well as 70% coarse-grained bainite and 30% fine ferrite in the base metal. They concluded that very large grains located around porosities were responsible of the reduction in toughness and ductility of the joints. Musa et al. [12] studied the effect of GTAW parameters on the evolution of the microstructure and microhardness in a L450 HSLA steel. They demonstrated that the welding parameters heat input led to an increase in the width of the HAZ and growth of prior austenite grains. Oyyaravelu et al. [13] investigated the influence of LBW parameters on the

microstructure and mechanical properties for SA516 grade 70 boiler steel. They revealed a strong correlation between welding parameters, final microstructure, and mechanical properties, where a martensitic structure was observed in the weld metal due to very high cooling rates. Fatigue properties in S500 welded specimens were investigated by Salabba et al. [14]. They confirmed that no distinct fatigue transition temperature was observed even at temperatures below the ductile–brittle transition temperatures obtained from Charpy impact and fracture toughness tests. Saha et al. [15] studied the evolution of the microstructure and mechanical properties for dissimilar dual-phase HSLA joined by LBW. Transmission electron microscopy revealed the microstructure of bainite in the dissimilar weld metal consisting of bainite ferrite embedded with intra-lath and inter-lath cementite precipitates. The obtained results indicated a correlation between the dispersion of multiple carbides inside the bainite/ferrite laths and the mechanical properties of the dissimilar joint such as ductile deformation and fracture behavior. Ribeiro et al. [16] studied the influence of the LBW heat input on the mechanical and microstructural properties of the welding zones for HSLA ferritic-pearlitic steel. Results confirmed that microstructural properties are governed by heat input, where high heat input promotes the formation of acicular ferrite, Widmanstätten ferrite, and grain boundary ferrite, while formation of martensite and bainite rather occurred using a low heat input. Kornokar et al. [17] investigated the effects of heat input during gas tungsten arc welding (GTAW) on the microstructure and mechanical properties of S500MC steel. Increasing heat input resulted in changes to the microstructure, including larger martensitic packets and increased retained austenite. The heat-affected zone (HAZ) showed two regions: coarse grain HAZ (CG-HAZ) and fine grain HAZ (FG-HAZ). Despite microstructural changes, the tensile strength remained unaffected, reaching a maximum of 690 MPa. The presence of martensite in the weld metal contributed to its increased strength, leading to failure in the base metal rather than the weld zone. Recently, Moradi et al. [18] used LBW to fabricate tensile specimens of HSLA-S500MC steel by applying different heat inputs. They demonstrated that LBW process may negatively affect the mechanical properties of the joint due to a heterogeneous microstructure produced by the controlled thermomechanical processing stage. However, by using low heat input, the tensile properties are more satisfactory and closer to the base metal.

Since the unique mechanical properties of HSLA steels are derived from controlled thermomechanical processing stage, there is concern that during the welding process, the properties created by the controlled thermomechanical process would be lost. Therefore, it seems necessary to choose

a welding process that can limit the undesirable properties of the HAZ. The choice of welding method depends on various factors such as desirable mechanical and microstructural properties, financial considerations, and flexibility. Although the choice of welding process is important, few studies have been done in regard to contrast the joint properties of HSLA steels obtained from different welding methods. This research is an attempt to compare and contrast the joint properties of HSLA-S500MC steel welded by LBW and GTAW methods.

2 Materials and methods

In this research, the material under study is S500MC steel from the family of high-strength low-alloy steel (HSLA). S500MC is manufactured according to DIN EN10149-2 standard [19] by thermomechanical process (with controlled heating and cooling cycles) in order to develop higher strength, toughness, and formability. HSLA-S500MC steel samples with dimensions (60 × 30 × 1.3 mm) were used as the base metal. A quantitative chemical composition test was performed on the S500MC samples and results are compared with standard composition limits as shown in Table 1. S500MC steel typically does not contain high levels of aluminum. But in this case, the max of Al should be lower than 0.015%. The high percentage of Al (0.054%) can lead to the formation of aluminum oxide, which can hinder proper fusion and reduce weld quality. Aluminum may increase the susceptibility to weld cracking, particularly hot cracking or solidification cracking.

Prior to welding, the plates were grounded and cleaned using acetone to remove surface oxides before to be clamped in a butt-joint configuration without gaps. The LBW welding processes include a fiber heat source and GTAW process is conducted by automatic carrying torch system in order to increase the stability and consistency of the welding process. The welding operation was performed in autogenous mode for both processes. The laser welding operation was done in

one pass using a fiber laser with a maximum average power of 300 W in a continuous mode. Before the welding process, the specimens were cleaned with acetone, and 99.9% pure argon gas was used to remove surface contaminants with a flow rate of 12 L/min. The gas was manually disconnected and connected after each sample to prevent wastage. To protect the weld pool, 99.9% pure argon gas was used during the welding process. The joint design for both welding processes was butt design.

The distance between the nozzle and the surface of the workpiece was set at constant value of 12 mm for all tests so that the focal plane position was kept at the middle of the thickness of the samples which is 0.75 mm below the surface.

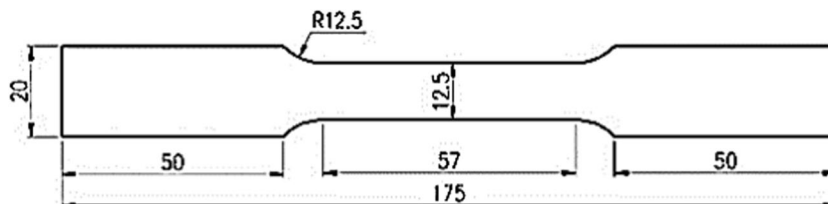
An automatic GTAW system was used on an adjustable welding table. The tungsten electrode (Ø3.2 mm) contained 2% thorium. The angle of the welding torch was set at 60° relative to the horizontal surface. GTAW operation was performed with direct current electrode negative (DCEN) for less spatter and a more stable arc using constant-voltage power source with argon as the shielding gas at a flow rate of 10 L/min for proper coverage.

After welding, metallographic samples were mounted in Bakelite, polished to 2500 grit and then using 1 µm diamond paste, and finally chemically etched using Nital solution (2%) during 8 s. Metallographic analysis was performed by an Meigi optical microscope and a VEGA TESCAN-XMU scanning electron microscope. Mechanical properties of the joints were obtained from tensile test specimens which were machined from the cross section of the welded samples using a wire-EDM and subjected to tensile testing according to the ASTM-E8 standard as presented in Fig. 1 with a Kopa machine. The tensile tests were performed at a speed of 2 mm/min at room temperature. In addition, a hardness test was performed to evaluate the hardness changes from the welding area to the base metal according to the ASTM E18 standard with a force of 100 kg and a force application time of 15 s at room temperature.

Table 1 Quantometric chemical test results of S500MC based on weight percentage of elements (wt. %)

	C % max	Mn % max	Si % max	P % max	S % max	Al % max	Nb % max	V % max	Ti % max
DIN EN10149-2	0.12	1.7	0.5	0.025	0.015	0.015	0.09	0.2	0.15
Quantometric test	0.105	1.644	0.133	0.009	0.001	0.054	0.007	0.004	0.003

Fig. 1 ASTM-E8 standard test specimen [20]



In this study, six different samples were considered for each welding methods (i.e., six different welding process parameters to generate different heat inputs for each process). Since this metric is almost impossible to measure experimentally, the amount of heat input in LBW and GTAW was assessed using the following Eq. (1) and Eq. (2):

$$Q_{LBW} = \frac{60 * P}{S} \quad (1)$$

$$Q_{GTAW} = \frac{60 * V * I}{S} \quad (2)$$

where Q is the heat input (J/mm), P is the laser beam power (W), V is the welding voltage (V), I is the welding current (A), and S is the linear welding speed (mm/min). Table 2 shows the specific parameters used to produce the 12 samples. For six LBW samples focal plane position of -0.75 mm and for six GTAW samples, voltage of 21 V was used during joining operation.

3 Results and discussion

3.1 Effect of process parameters on microstructure

Figure 2 presents the optical microstructure of the LBW and GTAW joints consists for heat input of 240 J/mm and 1995 J/mm respectively. The microstructure of the LBW samples is composed of acicular ferrite with some retained austenite as presented in Fig. 2a, while the one by the GTAW process consists of coarse acicular martensite, which are often surrounded by a significant amount of retained austenite (Fig. 2b). The mechanical properties of the material in LBW and GTAW welding processes are dependent on the microstructure. The heat input during welding processes is one of the factors that can affect the resulting microstructure and, consequently, the mechanical properties of the welded material. Since each sample has a distinct and different heat input, this difference in heat input has affected the size of the martensite packets and the amount of retained austenite. As the heat input increases, the cooling rate decreases and a growth of martensite packets is expected. In samples with low heat input, the opposite happens and as a result, a finer microstructure is obtained.

Table 2 LBW and GTAW process parameters

Sample No	LBW input parameters			GTAW input parameters		
	Laser power (W)	Welding speed (mm/min)	Heat input (J/mm)	Current (A)	Welding speed (mm/min)	Heat input (J/mm)
1	300	200	90	105	75	1764
2	300	150	120	95	60	1995
3	350	150	140	105	65	2035
4	270	100	162	110	65	2132
5	270	75	216	115	65	2229
6	300	75	240	120	65	2330

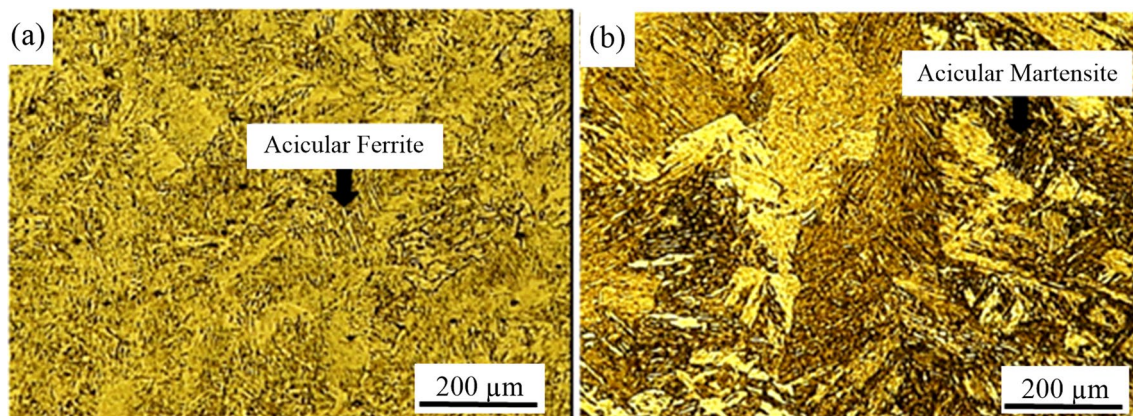


Fig. 2 Microstructure of weld metal for (a) heat input of 240 (J/mm) by LBW and (b) heat input of 2330 (J/mm) by GTAW

Figures 3 and 4 show the microstructure of the triple zones of BM, HAZ, and WZ by GTAW and LBW. The base metal is manufactured by thermomechanical operation (heat treatment—hot rolling) and subjected to normalizing heat treatment, which resulted in a very fine-grained ferrite-pearlite microstructure. Figures 3(c) and 4 (c) show the fine-grained heat-affected zone (FG-HAZ) of both welding processes. The FG-HAZ is the area which exceeds A_{c3} temperature. FG-HAZ in the LBW joint sample has a

ferrite + martensite microstructure, the formation of these two phases next to each other is a sign of dual-phase (DP) steels. Due to the high heat concentration of the LBW during process, the temperature of the FG-HAZ does not exceed the temperature range of 723–911 °C and the austenite phase transforms into martensite through a high cooling rate. Figure 3(d) shows the coarse-grained heat-affected zone (CG-HAZ) resulting from LBW welding, and Fig. 4(d) shows the same zone from automatic GTAW process. The

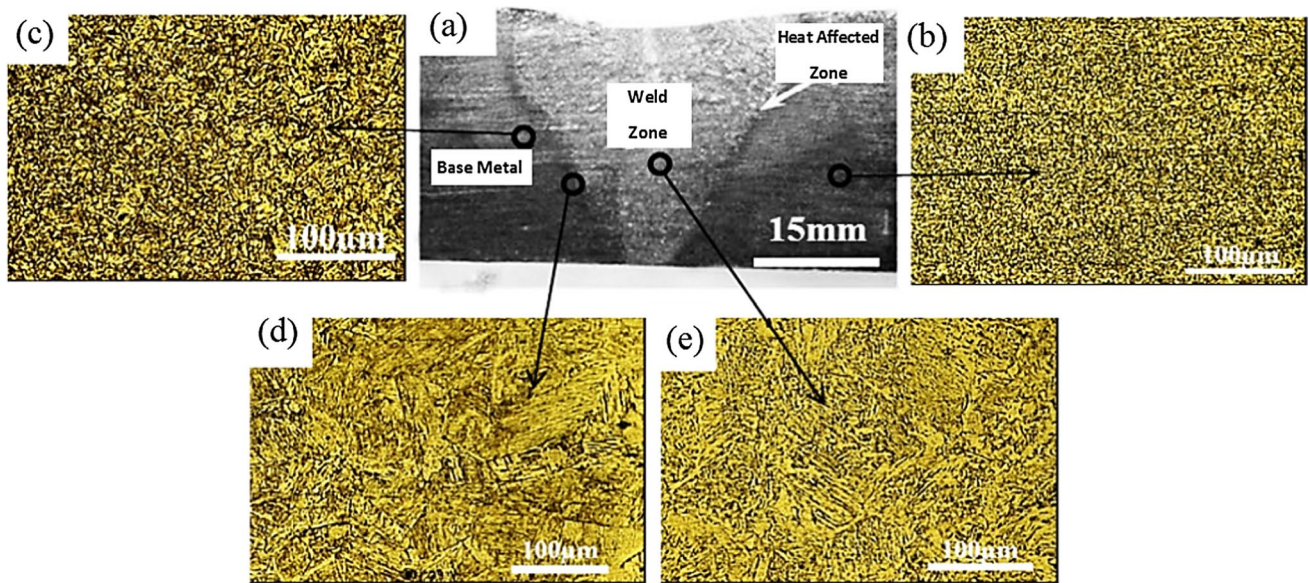


Fig. 3 (a) Macrostructure of LBW joint cross section, (b) microstructure of base metal, (c) microstructure of the fine-grained heat-affected zone (FG-HAZ), (d) microstructure of the coarse-grained heat-affected zone (CG-HAZ), and (e) microstructure of the weld metal

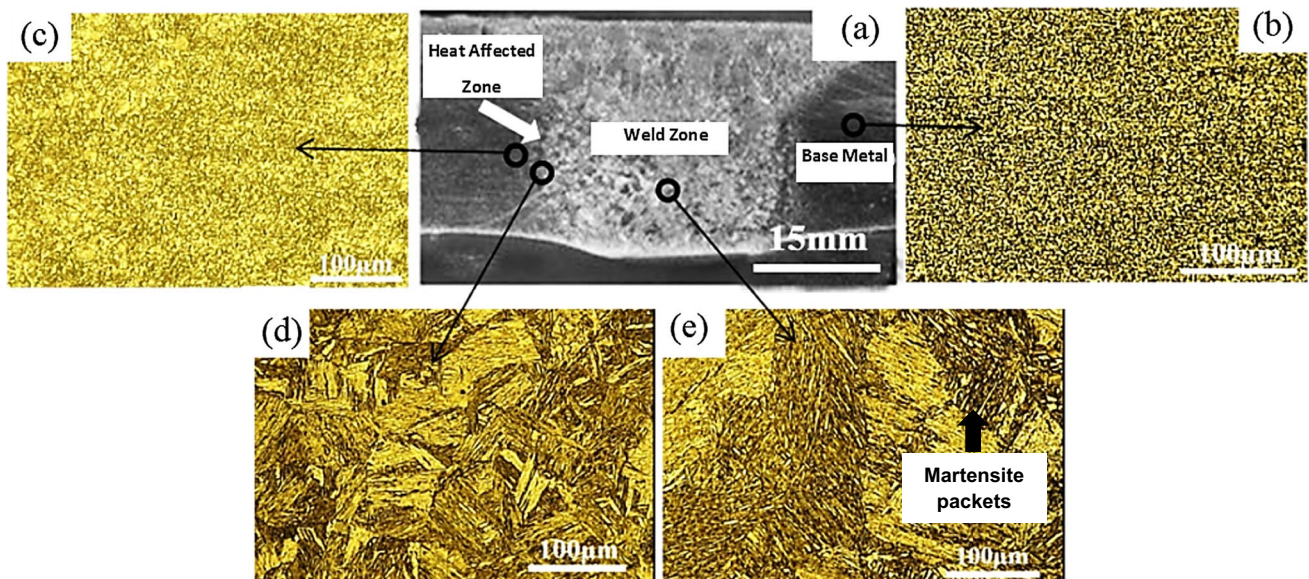


Fig. 4 (a) Macrostructure of automatic GTAW joint cross section, (b) microstructure of base metal, (c) microstructure of the fine-grained heat-affected zone (FG-HAZ), (d) microstructure of the coarse-grained heat-affected zone (CG-HAZ), (e) microstructure of the weld metal

microstructure of CG-HAZ is similar in both welding processes and includes acicular (needle-shaped) martensite surrounded by some retained austenite. Figure 3(e) shows the microstructure of the weld metal. The microstructure consists of acicular ferrite with retained austenite and locally formed martensite in some places. Figure 3(e) shows the same zone in GTAW process. The microstructure of GTAW metal pool consists of needle-shaped martensite surrounded by a small amount of retained austenite. Since the force of the plasma jet in the electric arc welding is the main cause for mixing of the weld pool, in the welding process by the electric source, the weld pool benefits from the mixing of the alloying elements. With a uniform distribution of alloying elements, if the base metal is hardened or the cooling rate is fast enough, the martensite transformation occurs, which can be seen in Fig. 4(e) for automatic GTAW process. In the LBW process, although the cooling rate is higher than that in GTAW welding, the martensitic microstructure is not formed, which seems to originate from the lack of plasma jet force in the laser weld pool. Despite the lack of sufficient mixing force in the weld pool, martensite forms in areas with more carbon and acicular ferrite in areas with less carbon. The important point to remember that the high temperature range and the high velocity flow of the plasma leads to intense chemical reactions and mixing in the weld pool [21].

Figure 5 (a) and (b) show the SEM images of FG-HAZ in automatic LBW and GTAW processes. The microstructure created in the FG-HAZ of the laser welding has better morphological properties than the base metal, while the microstructure of the same zone in the automatic GTAW process includes ferrite + pearlite and martensite. Since in GTAW the cooling rate is relatively slow, part of austenite phase transforms into pearlite the rest into martensite.

Figure 5(c) and (d) show the SEM images of the CG-HAZ in both processes, which indicates that the size of the martensite packets in the LBW process is much finer than in automatic GTAW, which can be justified by considering the LBW heat input to be about 10 times lower compared to automatic GTAW. Different welding heats in HAZ and WZ with different cooling rates have caused dissimilar metallurgical transformations to occur in the LBW and GTAW processes. The occurrence of martensitic microstructure in LBW can be related to the good hardenability of HSLA metal. The presence of alloying elements in base metal composition has hardened the steel, so that a martensitic microstructure is formed in the HAZ despite low cooling rate. To obtain an estimation of the cooling rate in welding processes, several parameters must be taken into account. The heat input signifies the magnitude of heat energy introduced into the weld. The welding speed governs the rate at which the welding torch traverses the joint. Material properties, including specific heat capacity and density, play a pivotal role as they dictate the heat absorption and retention

characteristics of the material. Moreover, the geometric dimensions of the specimen, encompassing length, width, and thickness, define the volume of the weld and resulting mass. The estimation of the cooling rate necessitates a systematic procedure. Initially the mass of the weld must be determined by multiplying the volume of the specimen by the material density. The energy delivered to the weld is roughly computed by multiplying the heat input by the welding speed and the mass. The temperature change is derived by dividing the energy delivered by the product of the mass and the specific heat capacity. Finally, the cooling rate is obtained by dividing the temperature change by the cooling time.

3.2 Effect of process parameters on mechanical properties

3.2.1 Hardness properties

In order to investigate the hardness changes across the joint in the WZ the HAZ and the base metal, a hardness test has been performed, and the profile of the hardness changes in the cross section of the LBW sample and the automatic GTAW sample based on the distance from the weld center is shown in Fig. 6. As can be seen in this figure, the hardness of LBW weld metal is lower than the hardness of GTAW weld zone. This difference in the weld metal is caused by the difference in microstructure, so that the laser fusion zone with acicular ferrite microstructure shows less hardness than GTAW weld metal with martensitic microstructure. According to the figure, the hardness values in the HAZ of both processes are almost the same, as these two zones have almost the same morphology, including martensite and retained austenite. Of course, the size of the martensite packets in the HAZ in the LBW process is smaller because the heat input is lower and the cooling rate is higher, but it still shows the same hardness as the GTAW heat-affected zone. The hardness results of these two welding methods show that the average hardness of the GTAW fusion zone is about 266 Vickers and also for the LBW sample it is 243 Vickers. In general, the hardness values in the GTAW fusion zone are about 8.5% higher than those in the same zone in the LBW sample. According to the figure, the width of GTAW fusion zone is about 5 mm, while the width of LBW weld metal is about 2 mm, and the thickness of the HAZ in GTAW sample is about 11 mm, and the thickness of the same zone in LBW sample is about 3 mm.

3.2.2 Tensile properties

The mechanical properties obtained from the tensile tests are articulated in Fig. 7 including ultimate strength, yield strength, and elongation at break. Figure 7(a) describes

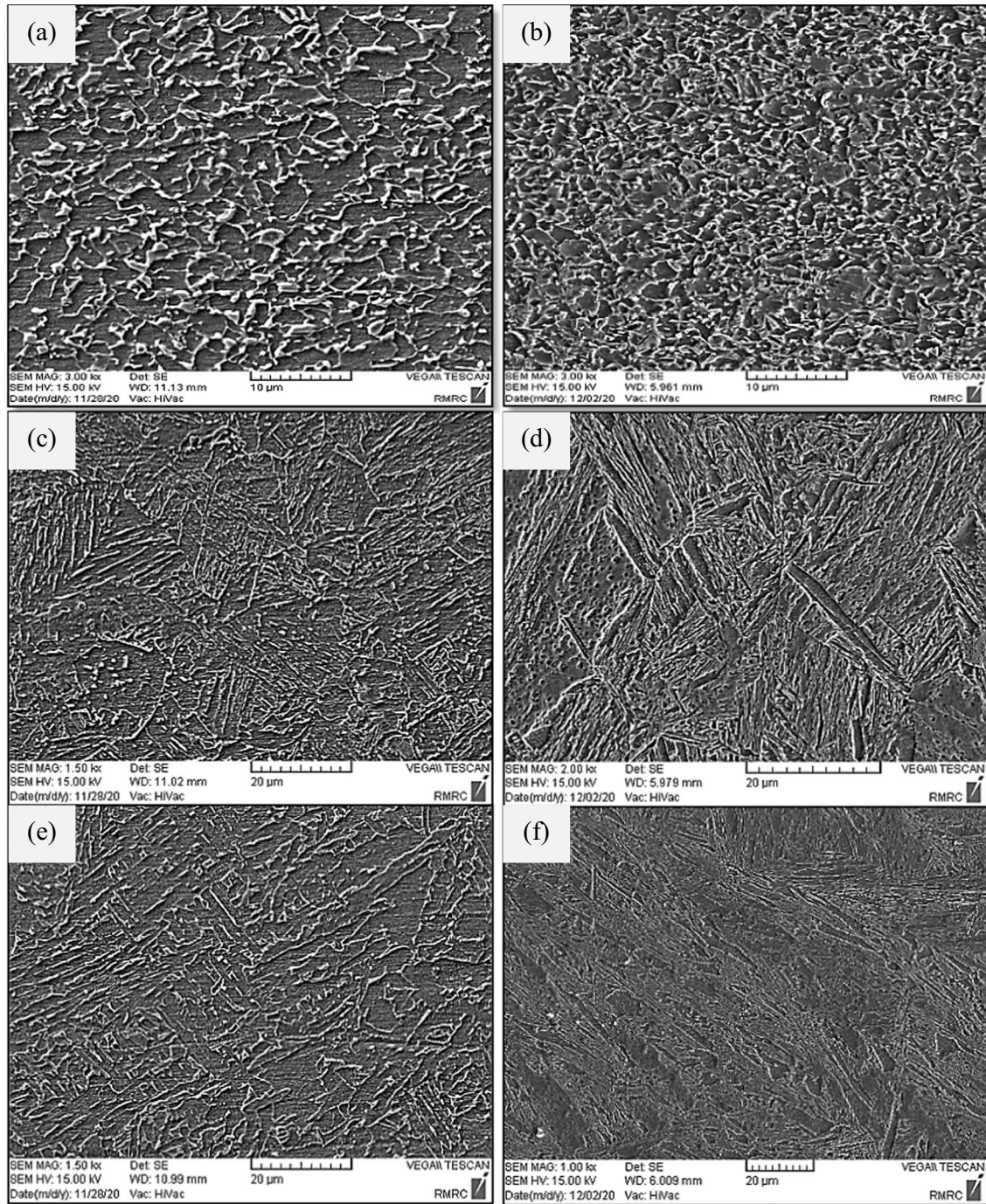


Fig. 5 SEM images of (a) FG-HAZ by LBW process, (b) FG-HAZ by GTAW process, (c) CG-HAZ by LBW process, (d) CG-HAZ by GTAW process, (e) weld metal by LBW process, (f) weld metal by GTAW process

the joint properties obtained by LBW. The first point that appears is that the heat input has almost similar effects on the ultimate strength and the yield strength of the LBW joint and produces almost the same trends. The next point is that lower heat input creates higher strength in the joint. Although the strength of the joint is increased again with further increase of the heat input, but this increase in the

strength at high heat input has other side effects such as increasing the width of the HAZ that are not desirable.

Figure 7(b) shows the effect of heat input on the elongation at break in the LBW joint. This figure is of great importance because information about the effect of heat input on the toughness of the joint can also be obtained from this figure. As shown in the figure, there is a value for

Fig. 6 Comparison of hardness profile in cross section of LBW and automatic GTAW samples

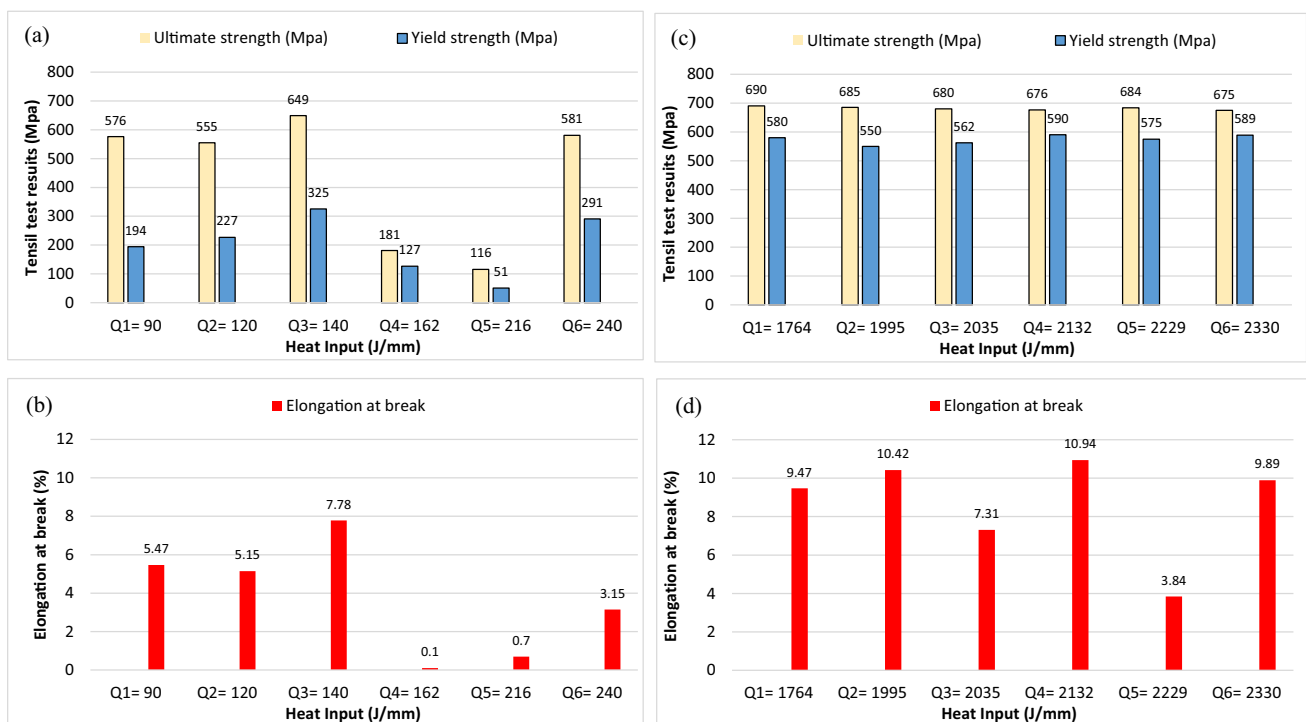
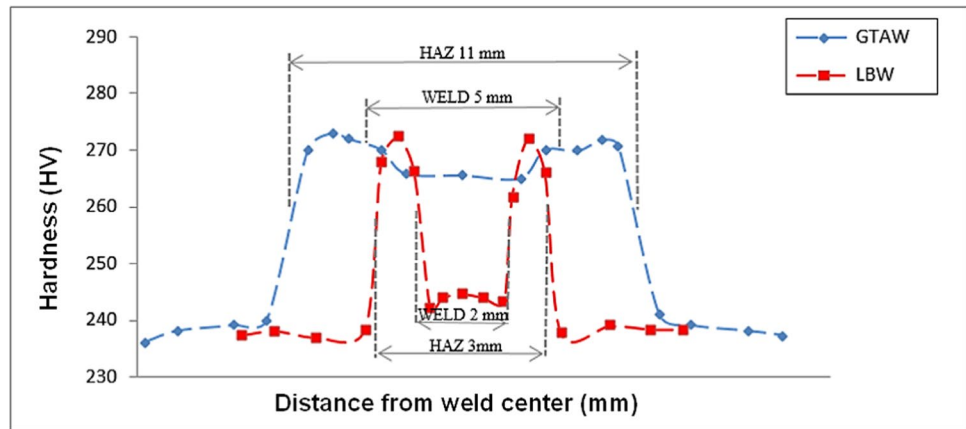


Fig. 7 (a) Diagram of the ultimate strength and yield strength of samples welded by LBW, (b) diagram of the elongation at break of samples welded by LBW, (c) diagram of the ultimate strength and yield

strength of samples welded by GTAW, (d) diagram of the elongation at break of samples welded by GTAW

the heat input in which the maximum elongation at break is created. A comparison of Fig. 7(a) and (b) shows that heat input of 140 (J/mm) produces the highest strength and elongation at break in the LBW joint at the same time yielding the maximum joint toughness.

Figure 7(c) shows the effect of heat input on the ultimate strength and yield strength of the joint by GTAW. It should be noted that because the failure occurred in all these specimens from the base metal, these graphs actually represent the mechanical properties of the base metal.

Figure 7(d) shows the effect of heat input on elongation at break in GTAW joint. As indicated, this diagram actually depicts the properties of the base metal, and it is not possible to draw a specific conclusion on the effect of heat input on elongation at break.

As expected, the results presented in Table 3 confirm that weld joints exhibited lower static mechanical strengths than that of the base metal. Although both welded joints exhibited similar ultimate strengths, the GTAW specimens demonstrated a significantly higher yield strength as compared to LBW

Table 3 Tensile test results of base metal, and LBW and GTAW samples

Sample	Yield strength (MPa)	Ultimate strength (MPa)	Strain (%)
Base metal	565	662	13.9
LBW	325	649	9.78
GTAW	580	690	9.47

joints (i.e., more than 50% higher). The low yield strength exhibited by the LBW specimens is probably explained by presence of ferrite (instead of martensite) within the WZ, leading in a failure in the WZ for such joints. Note that the presence of martensite in the WZ of the GTAW specimens has moved the failure location within the BM for the GTAW specimens. Therefore, the strength of the GTAW specimen is higher than the LBW specimen and even the base metal. In other words, in GTAW specimen the ultimate strength is 4.2% and the yield strength is 2.6% than the base metal.

When laser welding of S500MC steel, the resulting welded joint's microstructure and mechanical properties are affected by various processing parameters, including heat input. The figures suggest that certain amount of the heat input leads to an enhancement in the ultimate strength and yield strength, of the welded joint. However, it is important to note that the appropriate heat input may vary depending on the specific welding method employed and the desired mechanical property.

4 Conclusions

The results obtained in this study include LBW and automatic GTAW processes on S500MC steel in autogenous mode as follows:

- By changing the heat input in each welding process, the morphology of the microstructure is almost the same and only the size of the grains and the amount of remaining austenite change. In other words, the hardenability of steel dominates the cooling rate, and depending on the type of process, the same microstructure is formed at all heat inputs. Of course, in the samples with the lowest heat input, a fine microstructure with a larger volume of retained austenite is created, which results in better mechanical properties.
- Fusion welding of S500MC steel without the use of filler metal destroys the properties resulting from thermomechanical operations and metallurgical transformations occurs in all zones under welding. In this research, the joint obtained from the GTAW process shows better results in the mechanical properties than the joint obtained from the LBW process.

- GTAW sample strength is much higher than LBW samples and laser welded samples will fail from the welding zone under transverse loading. While in GTAW process, the welding strength is higher and it does not break from the joint location.
- The hardness values in the HAZ of both welding methods were almost the same, but in the weld zone, the hardness depends on the type of microstructure and grain size. The hardness value of weld metal of GTAW is about 8.5% higher than LBW samples.
- Distortion of parts in GTAW process is significant, but this value was insignificant in LBW. Therefore, LBW is a suitable option to avoid distortion in the sample.

Author contribution **Saleh Meiabadi**: formal analysis, software, writing — original draft. **Fardin Nematzadeh**: conceptualization, methodology, data curation, visualization, supervision, validation, resources, writing — review and editing. **Kianoosh Kornokar**: methodology, experiments, formal analysis, project administration. **Hossein Mostaan**: investigation, supervision, writing — review and editing. **Mahmoud ShamsBorhan**: methodology, data curation, visualization, resources. **Rasoul Khandan**: writing — review and editing, resources, methodology. **Vincent Demers**: writing — review and editing, formal analysis, software. **Jonathan Lawrence**: supervision, writing — review and editing, resources, formal analysis, methodology. **Mahmoud Moradi**: supervision, writing — review and editing, resources, methodology, formal analysis, validation.

Data availability The authors confirm that all data generated or analyzed during this study are included in this article.

Declarations

Conflict of interest The authors declare no competing interests.

Open Access This article is licensed under a Creative Commons Attribution 4.0 International License, which permits use, sharing, adaptation, distribution and reproduction in any medium or format, as long as you give appropriate credit to the original author(s) and the source, provide a link to the Creative Commons licence, and indicate if changes were made. The images or other third party material in this article are included in the article's Creative Commons licence, unless indicated otherwise in a credit line to the material. If material is not included in the article's Creative Commons licence and your intended use is not permitted by statutory regulation or exceeds the permitted use, you will need to obtain permission directly from the copyright holder. To view a copy of this licence, visit <http://creativecommons.org/licenses/by/4.0/>.

References

1. Bagchi A, Saravanan S, Kumar GS, Murugan G, Raghukandan K (2017) Numerical simulation and optimization in pulsed Nd: YAG laser welding of Hastelloy C-276 through Taguchi method and artificial neural network. *Optik* 146:80–89

2. Meiabadi MSSM, Kazerooni A, Moradi M, Torkamany MJ (2020) Laser assisted joining of St12 to polycarbonate: Experimental study and numerical simulation. *Optik* 208:164151
3. Moghanizadeh A, Honarvar F, Ghoreishi M, Ghajar R (2011) An investigation of the parameters affecting the quality of resistance spot welds in low carbon steel sheets. *Aerosp Mech J* 7(2):1–9
4. Mourad AI, Khoureshid A, Sharef T (2012) Gas tungsten arc and laser beam welding processes effects on duplex stainless steel 2205 properties. *Mater Sci Eng, A* 549:105–113
5. Xu J, Chen J, Duan Y, Yu C, Chen J, Lu H (2017) Comparison of residual stress induced by TIG and LBW in girth weld of AISI 304 stainless steel pipes. *J Mater Process Technol* 248:178–184
6. Fydrich D, Łabanowski J, Rogalski G, Haras J, Tomków J, Świerczyńska A, Jakóbczak P, Kostro Ł (2014) Weldability of S500MC steel in underwater conditions. *Adv Mater Sci* 14(2):37–45
7. Perka AK, John M, Kuruveri UB, Menezes PL (2022) Advanced high-strength steels for automotive applications: arc and laser welding process, properties, and challenges. *Metals* 12(6):1051
8. Verdeja JI, Asensio J, Pero-Sanz JA (2003) Texture, formability, lamellar tearing and HIC susceptibility of ferritic and low-carbon HSLA steels. *Mater Charact* 50(1):81–86
9. Blackman SA (1965) 2003 An economic assessment of mechanized welding of high-strength linepipe for the Australian pipeline industry. *Pipes Pipelines Int* 48(2):27–37
10. Ramirez JE (2008) Characterization of high-strength steel weld metals: chemical composition, microstructure, and nonmetallic inclusions. *Weld J New York* 87(3):65
11. Frih I, Adragna PA, Montay G (2015) Influence of a welding defect on a hsla s500mc steel plate: microstructure and residual stress evaluation. *Proceedings of the 6th International Conference on Mechanics and Materials in Design*. Editors: J.F. Silva Gomes, S.A. Meguid, P. Delgado/Azores, 26–30 July 2015, Paper ref: 5404, pp. 169–180
12. Musa MHA, Maleque A, Ali MMY (2018) An Investigation of TIG welding parameters on microhardness and microstructure of heat affected zone of HSLA steel. *IOP Conf Ser Mater Sci Eng* 290:12041
13. Oyyaravelu R, Kuppan P, Arivazhagan N (2016) Metallurgical and mechanical properties of laser welded high strength low alloy steel. *J Adv Res* 7:463–472
14. Sallaba F, Rolof F, Ehlers S, Walters CL, Braun M (2022) Relation between the Fatigue and Fracture Ductile-Brittle Transition in S500 Welded Steel Joints. *Metals* 12:385
15. Saha DC, Westerbaan D, Nayak SS, Biro E, Gerlich AP, Zhou Y (2014) Microstructure-properties correlation in fiber laser welding of dual-phase and HSLA steels. *Mater Sci Eng, A* 607:445–453
16. Ribeiro HV, Baptista CA, Lima MS, Torres MA, Marcomini JB (2021) Effect of laser welding heat input on fatigue crack growth and CTOD fracture toughness of HSLA steel joints. *J Market Res* 11:801–810
17. Kornokar K, Nematzadeh F, Mostaan H, Sadeghian A, Moradi M, Waugh DG, Bodaghi M (2022) Influence of heat input on microstructure and mechanical properties of gas tungsten arc welded HSLA S500MC steel joints. *Metals* 12(4):565
18. Moradi M, Kornokar K, Nematzadeh F, Mostaan H, Meiabadi S, Demers V, Lawrence J (2023) Microstructural and mechanical investigation on fiber laser welding of S500MC steel. *Sādhanā* 48(32)
19. DIN EN 10149-2 (2013) Hot rolled flat products made of high yield strength steels for cold forming. *Deutsches Institut für Normung*
20. ASTM E8 (2013) Standard test methods for tension testing of metallic materials. *American Society for Testing and Materials*
21. Yarmuch MAR (2005) Effect of welding parameters on the plasma transferred arc welding (PTAW) process for autogenous beads and 410SS-WC overlays. *Dissertation, University of Alberta*

Publisher's note Springer Nature remains neutral with regard to jurisdictional claims in published maps and institutional affiliations.